J Arid Land (2025) 17(4): 538–559
doi: 10.1007/s40333-025-0011-0; CSTR: 32276.14.JAL.02500110

Science Press Springer-Verlag

Diversification of flavonoid accumulation among ecotypes of *Agriophyllum squarrosum* (L.) Moq. in response to drought stress

ZHAO Pengshu[1,2,3], YAN Xia[1,4*], QIAN Chaoju[1,2], MA Guorong[5], FANG Tingzhou[1,2], YIN Xiaoyue[1,2], ZHOU Shanshan[1,2], LIAO Yuqiu[1,2,3], SHI Liang[1,2,3], FAN Xingke[1,2], Awuku IBRAHIM[1,2], MA Xiaofei[1,2]

[1] Key Laboratory of Ecological Safety and Sustainable Development in Arid Lands, Northwest Institute of Eco-Environment and Resources, Chinese Academy of Sciences, Lanzhou 730000, China;
[2] Key Laboratory of Stress Physiology and Ecology in Cold and Arid Regions of Gansu Province, Northwest Institute of Eco-Environment and Resources, Chinese Academy of Sciences, Lanzhou 730000, China;
[3] University of Chinese Academy of Sciences, Beijing 100049, China;
[4] Key Laboratory of Inland River Ecohydrology, Cold and Arid Regions Environmental and Engineering Research, Northwest Institute of Eco-Environment and Resources, Chinese Academy of Sciences, Lanzhou 730000, China;
[5] Gulang County Sand Prevention and Control Technology Promotion Center, Wuwei 733100, China

Abstract: *Agriophyllum squarrosum* (L.) Moq., commonly known as sandrice, is an annual medicinal plant prevalent in the dunes across China's deserts. A garden trial revealed that flavonoid content varies among sandrice ecotypes due to long-term local adaptation to water variability. To investigate how sandrice responds to drought stress through the molecular metabolic regulation of flavonoids, we employed transcriptomic and metabolomic analyses during a 9-d ambient drought stress, examining three ecotypes along a precipitation gradient. The three ecotypes located in Dengkou (DK) County, Dulan (DL) County, and Aerxiang (AEX) village of northern China, which had 137, 263, and 485 mm precipitation, respectively. Soil moisture content was 4.04% after drought stress, causing seedlings of the three sandrice ecotypes to display collapsed structures, yellowing leaves, wilting, and curling. Among these, DL exhibited superior drought tolerance, in which plant height increase (PHI) and leaf area (LA) were significantly higher than those of DK and AEX. Flavonoid-targeted metabolomics identified that rutin, isoquercitrin, and astragalin constituted over 95.00% of the 15 flavonoid metabolites detected. A total of 12 differentially accumulated flavonoids (DAFs) were found, with rutin being the most abundant (1231.57–2859.34 ng/100 mg fresh weight (FW)), showing a gradual increase along the precipitation gradient. Transcriptomic analysis revealed 14 common differentially expressed genes (DEGs) associated with flavonoid synthesis among the three ecotypes. Integrative analysis of DEGs and DAFs indicated that sandrice adapts to drought stress by activating different flavonoid synthesis pathways. In DK, the dihydrokaempferol-dihydroquercetin pathway, regulated by flavonoid 3'-monooxygenase (*CYP75B1*), likely enhances drought adaptation. In AEX, transcriptional repression by O-methylatransferase (*OMT*) shifts the metabolic flux from the quercetin-isorhamnetin pathway to the quercetin-isoquercetin-rutin pathway in response to drought. DL, the most drought-tolerant ecotype, appears to activate the naringenin-apigenin-luteolin route and employs a unique flavonoid accumulation pattern in response to drought stress. Our data reveal that flavonoid synthesis in sandrice is fine-tuned among ecotypes to cope with drought, offering valuable germplasm resources and evaluation methods for sandrice acclimation and providing insights into drought response in non-model plants.

Keywords: drought tolerance; ecotype; flavonoid; medicinal plant; rutin

*Corresponding author: YAN Xia (E-mail: yanxia@lzb.ac.cn)
Received 2024-08-26; revised 2025-01-25; accepted 2025-02-26

Citation: ZHAO Pengshu, YAN Xia, QIAN Chaoju, MA Guorong, FANG Tingzhou, YIN Xiaoyue, ZHOU Shanshan, LIAO Yuqiu, SHI Liang, FAN Xingke, Awuku IBRAHIM, MA Xiaofei. 2025. Diversification of flavonoid accumulation among ecotypes of *Agriophyllum squarrosum* (L.) Moq. in response to drought stress. Journal of Arid Land, 17(4): 538–559. https://doi.org/10.1007/s40333-025-0011-0; https://cstr.cn/32276.14.JAL.02500110

1 Introduction

Drought is the most serious stress for plants, which impacts on both crop yield and quality (Yang et al., 2023). In recent years, abnormal global climate change will require plants to face more frequent droughts (Easterling et al., 2000; Xie et al., 2015; Hao et al., 2018). Drought stress can compel plants to accumulate reactive oxygen species (ROS), which can damage cell membrane structure and impair normal cellular functions, including a decline in photosynthesis due to stomatal closure and a decrease in leaf area (Basu et al., 2016). For plants, to survive in drought stress environments, many secondary metabolites play important protective roles (Ghorbanpour and Varma, 2017; Yadav et al., 2021; Gautam et al., 2023; Lu et al., 2023). Flavonoids, as one of the most important plant secondary metabolites, could serve various physiological functions under drought stress, including promoting the production of osmotic adjustment substances and stomatal closure (Li et al., 2021; Gao et al., 2022), eliminating ROS damage, and replacing and protecting the antioxidant enzyme defense system (Samanta, 2011; Agati et al., 2012; Shomali et al., 2022) like superoxide dismutase (SOD), peroxidase (POD), catalase (CAT), and ascorbate peroxidase (APX) (Kim et al., 2017).

Flavonoids have three rings (C6-C3-C6) as their basic skeleton, and researchers generally classify it into seven subclasses: isoflavones, flavones, flavonols, anthocyanidins, flavanols, flavanones, and chalcones according to the oxidation degree of the central heterocycle (Shen et al., 2022). Flavonoid biosynthesis in plants is generated at the junction of the acetate and shikimate pathway (polyketide pathway) and starts with the general phenylpropanoid pathway (GPP). Then, various stable flavonoids were synthesized by a series of successive enzymes (Shen et al., 2022), including phenylalanine ammonia lyase (*PAL*), cinnamate 4-hydroxylase (*C4H*), p-coumaroyl coenzyme A ligase (*4CL*), and chalcone synthase (*CHS*). Molecular function studies have elucidated that these flavonoid-regulated genes can be involved in plant adaptation to drought stress. Such as overexpression of *C4H* in *Ipomoea batatas* (L.) Lam. improved drought resistance by regulating phenolic biosynthesis in transgenic tobacco (*Nicotiana tabacum* L.) plants (Wang et al., 2017). *Arabidopsis thaliana* (L.) Heynh. lines overexpressing *4CL* of *Gossypium hirsutum* L. were more tolerant to drought treatment, which was related to improving antioxidative enzyme activity, up-regulation stress-related genes, and inducing the biosynthesis of lignin content (Sun et al., 2020). In tobacco, overexpression *CpCHS* of Chinese cherry (*Cerasus pseudocerasus* Lindl.) improves drought resistance of tobacco by promoting flavonoid accumulation and inducing antioxidative enzyme production (Hou et al., 2022). In a word, the biosynthesis of flavonoids showed interspecific regulation under drought stress in model plants and cash crops, demonstrating their phytochemical diversity among species. Since flavonoids are widely used in medical and health fields for antioxidant, anti-inflammatory, anti-microbial, anti-tumor, anti-diabetic, etc. (Lv et al., 2023), it is still challenging and valuable to explore the response patterns of flavonoids among ecotypes for the precise development and application of medicinal plants.

As desert plants endure long-term survival in a multi-stress environment, they tend to accumulate higher levels of flavonoids (Gao et al., 2021; Li et al., 2023). However, it remains unclear whether desert plants that have grown in arid environments for extended periods possess a unique flavonoid biosynthesis mechanism to cope with drought stress. *Agriophyllum squarrosum* (L.) Moq., commonly known as sandrice, is an annual medicinal desert plant abundant in flavonoids (Yin et al., 2018; Zhou et al., 2021a). It is widely distributed in dunes across arid and semi-arid areas, where the annual mean precipitation ranges from 37 to 485 mm, and expected to be a model plant to study the accumulation of flavonoids in response to drought stress in the deserts (Zhou et al., 2021b; Zhao et al., 2023). Previous common garden trial of sandrice has

shown that the differences in flavonoid accumulation among different ecotypes are the result of long-term adaptation to *in situ* precipitation and temperature environment heterogeneity (Zhou et al., 2021a). Subsequently, further research elucidated that the accumulation of a couple of flavonoids is negatively correlated with the *in situ* precipitation gradient along natural populations (Fang et al., 2022). To further verify how sandrice responds to drought stress through the molecular metabolic regulation of flavonoids, it is necessary to conduct a multi-omics study of drought treatments in different ecotypes with precipitation gradient.

In this study, based on flavonoid-targeting metabolomics and transcriptomics analysis, we selected three ecotypes from different precipitation gradients, including arid land ecotype, plateau arid land ecotype, and semi-arid land ecotype, for conducting a 9-d drought treatment without watering. The main aims were: (1) to investigate the differences in flavonoids accumulation patterns among ecotypes of sandrice coping with drought stress; and (2) to reveal the molecular metabolic regulation mechanism of flavonoid synthesis responding to drought stress of sandrice, and the local adaptation of flavonoid synthesis among different ecotypes. This study will deepen knowledge on the physiological and metabolic process in sandrice in response to drought stress, promote the understanding of the regulation mechanisms of flavonoid synthesis among ecotypes responding to drought stress, and provide a theoretical basis for the further precise utilization and development of the medicinal value of different ecotypes in sandrice.

2 Materials and methods

2.1 Plant growth, drought treatment, and sample collection

The seeds of natural ecotypes of sandrice were collected from Dengkou (DK) County, Dulan (DL) County, and Aerxiang (AEX) Village of northern China in 2014 (Table 1), and consistently preserved in a seed cabinet to ensure their viability at a constant temperature of 20.00℃ and humidity of 5.00%. The three ecotypes have been growing in distinct environments for a long time, resulting in noticeable differences in their phenotypic traits (Yin et al., 2016a). The data on *in situ* environmental factors for the three ecotypes were downloaded from WorldClim (https://www.worldclim.org/), and displayed along with the phenotypic traits in Table 1. The annual mean precipitation of DK, DL, and AEX ecotypes is 137, 263, and 485 mm, respectively. In 2022, seeds of the three ecotypes were grinded with 1 mm diameter sand (the ratio of sand to seed is 2:1, v/v), and germinated overnight in a dark incubator at 25.00°C. The next day, the germinated seeds were sown in pots filled with sand and nutrient soil (9:1, v/v). After the cotyledons grew, pots were placed under artificially simulated climatic conditions: a photoperiod of 16 h/8 h (light/dark) with approximately 30.00%–50.00% relative humidity and a temperature of 25.00°C–30.00°C in the greenhouse at the Northwest Institute of Eco-Environment and Resources, Chinese Academy of Sciences. There was only one healthy plant with the same growing consistency maintained in each pot by removing extra plants. A total of 36 pots were divided into six groups (6 pots for each group), including three control groups (CDK, CDL, and CAEX) and three drought treatment groups (DDK, DDL, and DAEX). All plants were timely watered to maintain a suitable soil moisture content until 35 d after germination (vegetative stage).

Table 1 Native habitat environments and phenotypic characteristics of the three ecotypes

Ecotype	Collection site	Altitude (m)	Latitude	Longitude	Mean annual precipitation (mm)	Annual mean temperature (°C)	Phenotypic characteristics
DK	Dengkou	1050	40°22′42″N	106°59′37″E	137	8.31	Small seed size and short broad leaf
DL	Dulan	3130	36°25′25″N	98°07′25″E	263	3.40	Seed wing, long broad thick leaf, and large leaf area
AEX	Aerxiang	251	42°52′04″N	122°25′40″E	485	6.38	Large seed size and long thin leaf

Note: DK, Dengkou County; DL, Dulan County; AEX, Aerxiang Village.

Water was continuously provided for the control group plants while withholding it from the drought treatment groups for 9 d until a drought stress phenotype with leaf wilting was observed. At this time, above-ground tissue samples were randomly pooled from 6 plants in each group, immediately frozen in liquid nitrogen, and stored in refrigerator at –80.00°C. A total of 18 samples with 3 biological replicates of each treatment were analyzed.

2.2 Plant physiological and morphological measurements

Soil moisture content, leaf relative water content (RWC; %), actual photochemical quantum yield (Fv′/Fm′, a universal indicator of plant stress severity), above-ground biomass (AGB; g), plant height increase (PHI; cm), leaf area (LA; mm^2), stem diameter (STD; mm), and basal branch length (BBL; cm) were applied to evaluate drought resistance and physiological difference among the three ecotypes of sandrice. The soil moisture content of control and 3, 6, and 9 d after drought stress was monitored using a soil moisture sensor (Shun Koda TR-6, Beijing, China) at 9:00 am (LST). Fresh weight (FW; g), turgid weight (TW; g), and dry weight (DW; g) of four leaves from each sample were weighed immediately after being isolated from the plants, rehydrated in distilled water at 4.00°C for 24 h until fully turgid, and dried at 70.00°C for 72 h until constant mass, respectively. We calculated the leaf RWC according to the following formula: leaf RWC (%)=(FW–DW)/(TW–DW)×100.00% (Prasad et al., 2011). Fv′/Fm′ was measured using MultispeQ v.2.0 software (PhotosynQ LLC Co. Ltd., East Lansing, Michigan, USA). LA and STD of the plants were measured using PhenoAI air (AgriBrain Co. Ltd., Nanjing, China) and a digital vernier caliper (DL91150, deli Co., Ltd., Yuyao, China), respectively. AGB was weighed using a 1/10,000 electronic analytical balance. PHI and BBL were measured with a ruler. Physiological data with 6 biological replicates of each treatment were statistically analyzed by one-way analysis of variance (ANOVA) and *t*-test at 0.050 and 0.010 levels using IBM SPSS v.17.0 software (SPSS Inc., Armonk, New York, USA). Bar chart was generated using the GraphPad Prism v.8.2.0 software.

2.3 Metabolite extraction and analysis

Approximately 100 mg of samples were extracted with 2 mL of 70.00% v/v aqueous methanol using ultrasonic waves for 30 min at a time for a total of 2 h, and the mixed extracts were concentrated to nearly dry on a rotary evaporator at 35.00°C under reduced pressure. Before analysis, the residue was dissolved in 200 μL of 50.00% methanol/water solution and transferred to insert-equipped vials.

The sample extracts were analyzed using the ultra-performance liquid chromatography-mass spectroscopy (UPLC-MS) system including alkaloids, amino acids, catechins, flavones, flavone glycosides, phenolic acids, and theaflavins. The chromatographic separation was performed on a high strength silica (HSS) T3 (50.0 mm×2.1 mm, 1.8 μm, Thermo Fisher Scientific Waltham, USA) column using water plus 0.10% acetic acid solution and acetonitrile plus 0.10% acetic acid solution as solvent system at a flow rate of 0.3 mL/min. The gradient program was set as follows: 0.0 min, 90:10 v/v; 2.0 min, 90:10 v/v; 6.0 min, 40:60 v/v; 8.0 min, 40:60 v/v; 8.1 min, 90:10 v/v; and 12.0 min, 90:10 v/v. The column temperature 40.00°C, and the injection volume was 2 μL.

High resolution mass spectrometry (HRMS) data were recorded on a Q Exactive Hybrid Quadrupole-Orbitrap mass spectrometer (Thermo Fisher Scientific, Waltham, USA) equipped with a heated electrospray ionization source utilizing the single ion monitoring MS acquisition methods. The electrospray ionization source parameters were set as follows: spray voltage, –2.8 kV; sheath gas pressure, 40 arbitrary unit (arb); aux gas pressure, 10 arb; sweep gas pressure, 0 arb; capillary temperature, 320.00°C; and aux gas heater temperature, 350.00°C.

Data were acquired on the Q-Exactive using Xcalibur 4.1 (Thermo Scientific, Waltham, USA), and processed using TraceFinder™4.1 Clinical (Thermo Scientific, Waltham, USA). Quantified data were output in Excel software (Microsoft, Redmond, USA). Principal component analysis (PCA) and orthogonal partial least squares-discriminant analysis (OPLS-DA) were performed using the Metware Cloud, a free online platform for data analysis (https://cloud.metware.cn). The

differentially accumulated flavonoids (DAFs) are filtered by a variable importance in the projection (VIP) ≥1.00 and P<0.050. Venn and hierarchical cluster heatmap analysis were performed using the OECloud tools at https://cloud.oebiotech.com. The stacking chart was performed using the Wekemo Bioinclod tools at https://bioincloud.tech.

2.4 Ribonucleic acid (RNA) isolation and library preparation

We extracted total RNA from 18 sandrice above-ground tissue samples using the TRIzol reagent (Invitrogen, Carlsbad, USA) according to the manufacturer's protocol. RNA purity and quantification were evaluated using the NanoDrop 2000 spectrophotometer (Thermo Scientific, Waltham, USA). RNA integrity was assessed using the Agilent 2100 Bioanalyzer (Agilent Technologies, Santa Clara, USA). Then we constructed the libraries using the VAHTS Universal V6 ribonucleic acid sequence (RNA-seq) Library Prep Kit from Vazyme Biotech Co., Ltd., Nanjing, China. The transcriptome sequencing was conducted by OE Biotech Co., Ltd., Shanghai, China.

2.5 RNA sequencing and expressed genes analysis

The libraries were sequenced on a llumina Novaseq 6000 platform and 150 bp paired-end reads were generated. The raw sequencing files of transcriptomic data are now available in the national center for biotechnology information (NCBI) sequence read archive (SRA) database with the accession number PRJNA940574. Raw reads in FASTQ (FASTQ is a text-based format used to represent biological sequences with their quality scores) format were firstly processed using FASTQ and the low-quality reads were removed. The clean reads were mapped to the AEX genome using Hierarchical Indexing for spliced alignment of transcript (HISAT) software. The expression levels of each gene are represented by the fragments per kilobase million (FPKM) value. The FPKM of each gene was calculated and the corresponding read counts were obtained by high-throughout sequencing (HTSeq)-count, a Phyton module for analyzing high-throughput sequencing data. Differential expression analysis was performed using the DESeq2, an R language package for analyzing differentially expressed genes (DEGs) in high-throughput RNA-seq data. For identifying DEGs, P-value<0.050 and $|\log_2(\text{fold change})|\geq 1.000$ were set as the threshold. The P-value, obtained through a t-test, is used to assess the statistical significance of differences. However, the q-value is the adjusted value of the P-value, and a more stringent statistical measure than the P-value. Fold change represents the degree of change between an initial value and a final value, calculated as the ratio of the final value to the initial value. Log_2 (fold change) is used to measure the difference in gene expression intensity between a sample and its corresponding control sample. Kyoto encyclopedia of genes and genomes (KEGG) enrichment analyses were employed to recognize the biological role and function of DEGs. KEGG enrichment analysis bubble map was produced using the OECloud tools at https://cloud.oebiotech.com.

2.6 Conjoint analysis method

Correlation analysis heatmap was produced using OriginPro v.2023 software (OriginLab Corporation, Northampton, USA). The network diagram was generated using the Metware Cloud, with a Pearson's correlation coefficient r≥0.800. And its significance of difference at P<0.050 was calculated and screened by SPSS v.17.0 software. We created the KEGG pathway heatmap based on the upstream and downstream relationships of flavonoid synthesis genes and metabolites in the KEGG pathway database.

2.7 Quantitative real-time polymerase chain reaction (qRT-PCR) analysis

RNA extracted from CDK, DDK, CDL, DDL, CAEX, and DAEX was used to validate the transcriptome data by qRT-PCR. Three technical replications were performed for each biological replication. Primers were designed using Primer Premier v.5.0 software (Premier Biosoft, Palo Alto, USA) (Table S1). The mean values of *AsUBC22* and *AsPP2A* were used as the internal reference gene (Fang et al., 2023). Target genes were amplified using PerfectStart SYBR qPCR Supermix (TransGen Biotech, Beijing, China) and a Real-Time qPCR System (Mx3000P, Agilent

Technologies Co., Ltd., Santa Clara, USA). The $2^{-\Delta\Delta Ct}$ method was used to analyze the normalized expression of each sample. It represents the fold change in the relative expression level of the target gene compared with the internal reference gene.

3 Results

3.1 Morphological and physiological responses to drought stress in sandrice

After a 9-d drought treatment, remarkable phenotypic characters were observed in the above-ground tissues of the three ecotypes (Fig. 1a), including wilting and curling of leaves, and plants got shorter and collapsed. In the whole experiment, the soil moisture content of the control group maintained 25.00%. The average soil moisture content of the treatment group gradually decreased to 10.70%, 5.20%, and 4.04% on 3, 6, and 9 d after the drought, respectively (Fig. 1b). Under normal culture conditions, AGB was similar in CDK and CDL (Fig. 1c). PHI, LA, STD, and BBL were the highest in CDL (Fig. 1d–g), compared with CAEX and CDK, indicating that DL has greater above-ground biomass. After the 9-d drought treatment, compared with the respective control groups, LA, STD, and BBL were almost not significantly different in the three ecotypes, except for the BBL of AEX. However, AGB significantly decreased by 75.83%, 51.42%, and 52.54%, and PHI decreased by 94.00%, 52.58%, and 72.93% in DDK, DDL, and DAEX ecotypes, respectively. Additionally, under normal moisture supply, Fv′/Fm′, a universal indicator of plant stress severity, was the highest in CDL (0.73) and the lowest in CAEX (0.65). However, compared with the respective control group, Fv′/Fm′ significantly decreased by 51.46%, 49.21% and 34.44% in DDK, DDL, and DAEX, respectively (Fig. 1h). In addition, the leaf RWC was not significantly different among the control groups of the three ecotypes, while there was a significant decrease in the drought treatment group, compared with the respective control group, and leaf RWC was higher in DDL than in DAEX and DDK after 9 d treatment (Fig. 1i). In a word, DK and AEX were presented drought sensitive, while DL showed the strongest resistance to drought stress.

3.2 Variations of flavonoids among sandrice ecotypes under drought stress

The composition of 15 flavonoid-targeted metabolites and their contents are shown in Table 2, with their contents ranging from 0.01 to 2859.34 ng/100 mg FW. The total amount of these compounds varied from 3560.70 to 5225.33 ng/100 mg FW. Among them, the total flavonoid content in AEX was the highest under both CAEX and DAEX. The PCA of the metabolome data explained 37.40% (principal component; PC1) and 21.90% (PC2) of the variation (Fig. S1a). The three replicates of each treatment group were all within the 95.00% confidence interval. However, drought treatment and control of each ecotype were separated, implying that sandrice responded to drought stress by regulating flavonoid accumulation. As shown in Figure 2a, rutin, isoquercitrin, and astragalin were identified as the most abundant flavonoids in all groups, and these metabolites accounted for more than 95.00% of the total 15 flavonoids. The content of other metabolites was relatively low (Fig. 2a). The OPLS-DA showed q>0.900 for each ecotype (Fig. S1b–d), indicating that these models were reliable and stable and could be used to further screen DAFs. There was a total of 12 DAFs, including 7 DAFs (rutin, quercetin, dihydrokaempferol, dihydroquercetin, naringenin chalcone, astragalin, and apigenin) specific to individual ecotype, 4 DAFs (vitexin, isorhamnetin, epicatechin, and naringenin) shared by the two ecotypes, and 1 DAF (luteolin) shared by the three ecotypes (Fig. 2b). Rutin, the most abundant compound, showed a gradual increase with precipitation gradient (Table 2), and significant increase in AEX after drought stress (Fig. 2c). Isoquercitrin and astragalin showed decrease in DK and DL, but increase in AEX under drought stress. In DL, astragalin showed a significant decrease (Fig. 2c). Those results demonstrated the flavonoids accumulation of the three ecotypes was affected differently, and rutin might play an important role under drought stress.

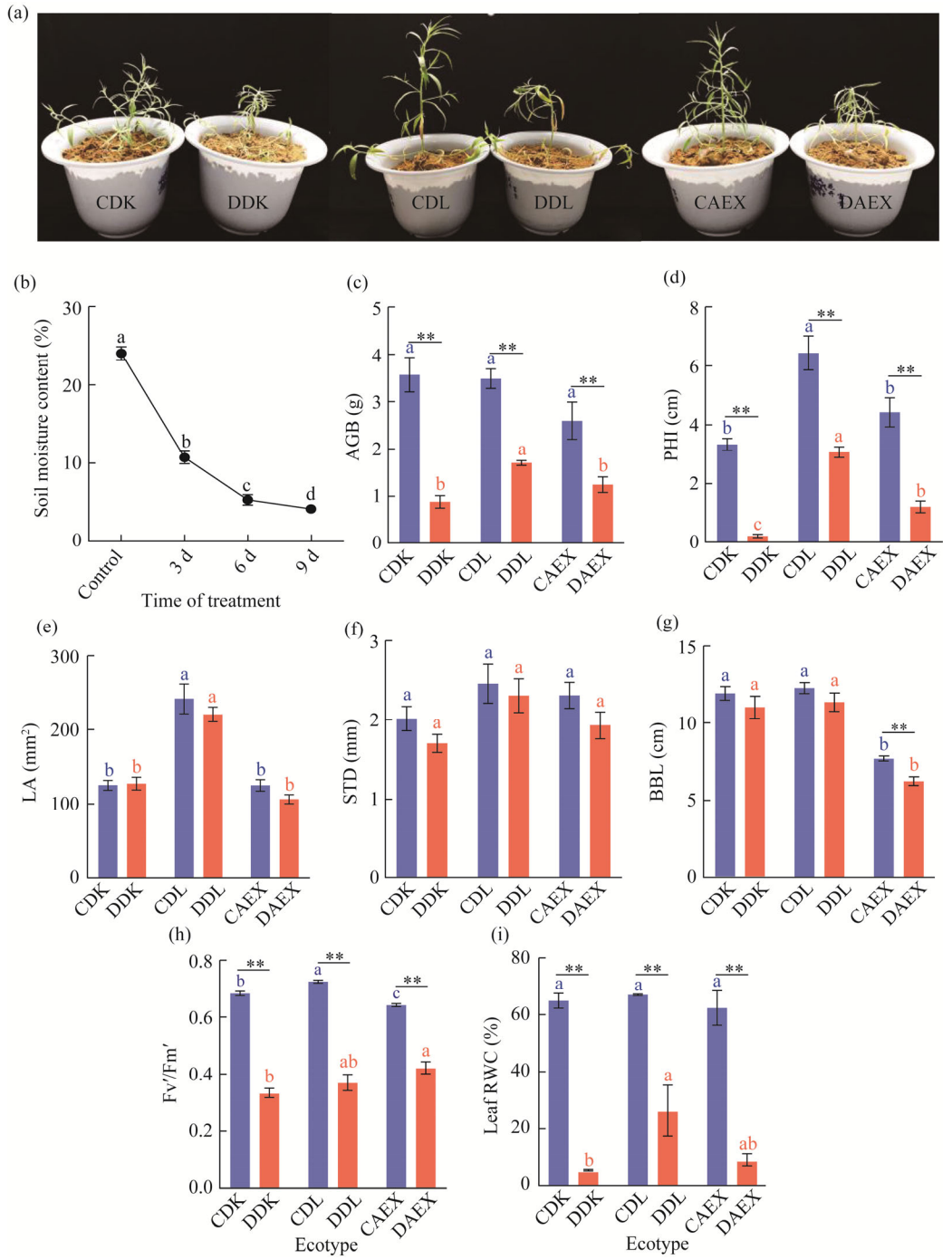

Fig. 1 Effects of drought stress on the morphological traits and physiological indicators in DK (Dengkou County), DL (Dulan County), and AEX (Aerxiang Village) ecotypes. (a), phenotype of DK, DL, and AEX after drought stress and control treatments (CDK, CDL, and CAEX); (b), soil moisture content; (c), above-ground biomass (AGB); (d), plant height increase (PHI); (e), leaf area (LA); (f), stem diameter (STD); (g), basal branch length (BBL); (h), Fv'/Fm' value at vegetative stage; (i), leaf relative water content (RWC). DDK, DDL, and DAEX represented the drought stress treatments of DK, DL and AEX, respectively. Bars are standard errors. Within the same treatment (control or drought), different lowercase letters indicated significant difference at $P<0.050$ level. Asterisks on shoulder lines indicated statistically significant differences between control and drought of the same ecotype. *, $P<0.050$ level; **, $P<0.010$ level. The abbreviations are the same in the following figures and tables.

Table 2 Composition and average content of 15 flavonoids targeting metabolites

Compound name	CDK	DDK	CDL	DDL	CAEX	DAEX
	(ng/100 mg fresh weight (FW))					
Rutin	1231.57	1350.47	1668.45	1720.60	2495.48	2859.34
Isoquercitrin	1653.85	1442.55	1726.87	1461.72	1577.22	1593.38
Astragalin	818.28	714.61	741.53	519.81	650.12	722.03
Quercetin	12.48	14.44	10.68	7.91	17.55	26.85
Vitexin	12.06	26.72	14.93	21.38	4.28	10.27
Isorhamnetin	3.45	5.82	2.01	1.99	12.88	5.27
Dihydrokaempferol	1.16	1.93	2.12	5.13	2.78	3.49
Kaempferol	2.17	1.59	1.73	1.52	2.63	2.13
Dihydroquercetin	1.02	1.24	0.85	1.49	1.09	0.97
Luteolin	0.38	0.55	0.65	1.72	0.45	0.89
Naringenin	0.39	0.50	0.45	1.75	0.18	0.49
Apigenin	0.11	0.13	0.10	0.14	0.08	0.08
Catechin	0.41	0.13	0.07	0.11	0.16	0.07
Epicatechin	0.10	0.01	0.11	0.01	0.03	0.06
Naringenin chalcone	0.56	0.01	0.82	0.68	0.01	0.01
Total flavonoid	3737.99	3560.70	4171.37	3745.96	4764.94	5225.33

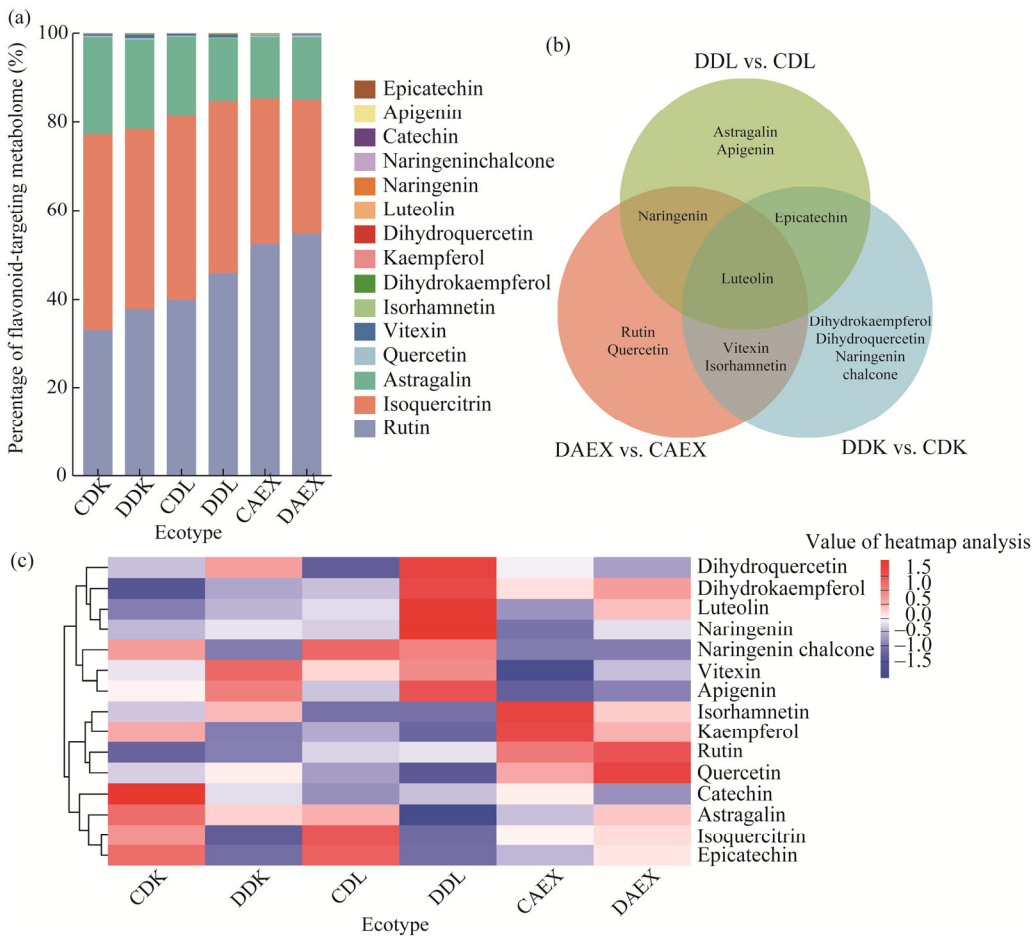

Fig. 2 Flavonoid-targeting metabolites identified in above-ground tissue of sandrice. (a), percentage of flavonoid-targeting metabolome; (b), Venn of metabolite significance analysis; (c), hierarchical cluster heatmap analysis of metabolites.

3.3 DEGs responding to drought treatment in sandrice

Total of 128.55 Gb raw reads from 18 samples were generated. After the removal of the low-quality reads, a total of 120.44 Gb clean data were retained for subsequent analyses. The total mapping rate was 95.68%–97.79% of each sample, and 92.19%–94.72% clean reads were uniquely mapped. Q30 (the percentage of bases with a mass value greater than or equal to 30) bases ranged from 90.54% to 91.92%, and the average GC (total proportion of guanine (G) and cytosine (C) bases in a DNA sequence) content was 44.69% (Table S2). The PCA of 18 samples was divided into the three ecotypes along PC 1, and control and drought treatments of each ecotype were separated along PC 2 (Fig. S2). CDK and CDL were closely grouped and were separated after drought treatment, indicating the response mechanisms to drought stress might be divergent.

DEGs analysis was performed between the control and drought treatments of the three ecotypes. A total of 3554, 1557, and 2374 up-regulated DEGs were identified in DK, DL, and AEX, respectively, while 4448, 2753, and 3594 down-regulated DEGs were identified (Fig. 3a). In the three ecotypes, the number of down-regulated DEGs was higher than that of up-regulated DEGs, and the total number of DEGs was the lowest in DL, indicating that DL was more stable than DK and AEX under drought stress. The Venn diagram showed 2584, 383, and 808 DEGs were unique

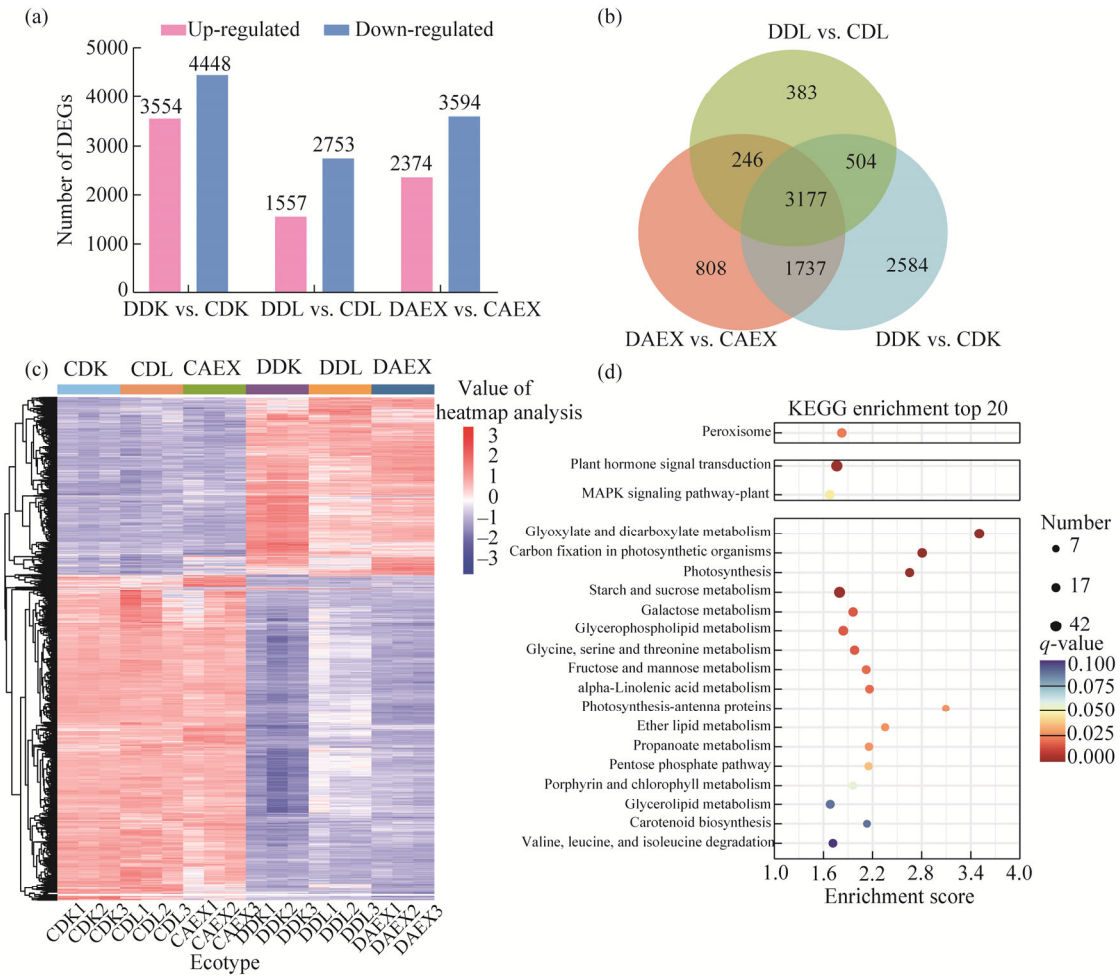

Fig. 3 Description of differentially expressed genes (DEGs) in transcriptome data of the three ecotypes of sandrice in response to drought. (a), number of DEGs; (b), Venn diagram showing overlap of DEGs in the three ecotypes; (c), heatmap analysis of 3177 DEGs in Figure 3b; (d), Kyoto encyclopedia of genes and genomes (KEGG) enrichment analysis bubble map. Dot size represents the number of distinct genes, and dot color reflects the *q*-value.

to DK, DL, and AEX, respectively (Fig. 3b). Among the common 3177 DEGs of the three ecotypes, there were 1118 up-regulated and 2020 down-regulated DEGs (Fig. S3a–b). Clustering heatmap of the shared DEGs visually presented the difference between drought and control groups (Fig. 3c). KEGG enrichment analysis bubble map showed the top 20 metabolic pathways of these common DEGs (Fig. 3d), including peroxisome, plant hormone signal transduction, starch and sucrose metabolism, glyoxylate and dicarboxylate metabolism, carbon fixation in photosynthetic organisms, and photosynthesis, indicating that the three ecotypes respond to a drought stress environment by producing plant hormones, regulating cellular processes and metabolic pathways, and synthesizing metabolites. To be mentioned, we noticed that flavonoids biosynthesis pathway did not show a common trend to respond to drought treatment, however, the bubble map of KEGG in different ecotypes showed that flavonoids biosynthesis was triggered by drought in DL (Fig. S4).

3.4 Integrative analysis of DAFs and DEGs

To further study the difference in flavonoid synthesis between different ecotypes, we found 14 DEGs in the three ecotypes related to flavonoid biosynthesis (Fig. 4a), with 8 DEGs being down-regulated under drought stress. To our surprise, the expression of some genes was different among the three ecotypes. 3'*GT* (anthocyanin 3'-O-beta-glucosyltransferase) was up-regulated in AEX, but down-regulated in both DK and DL, while *COMT*5 (caffeic acid 3-O-methyltransferase) was down-regulated in AEX and up-regulated in DK and DL. These results demonstrated that 3'*GT* and *COMT*5 had expression specificity and complementary trends among different genetic lineages.

Correlation analysis between DEGs and DAFs under drought stress showed that astragalin was significantly decreased in DL, which was negatively correlated with *CHI* (chalcone isomerase), *COMT*5, and *COMT*6, while positively correlated with *LDOX* (leucoanthocyanidin dioxygenase), 3′*GT*, *CYP*75*B*1 (flavonoid 3'-monooxygenase), *CHS* (chalcone synthase), and *ANR* (anthocyanidin reductase) (Fig. 4c). Rutin had a significant accumulation in AEX, which was negatively correlated with *AOMT*2 (flavonoid 3′,5′-methyltransferase), *CYP*75*B*1, *COMT*5, and *ANR*, while positively correlated with 3′*GT*, *FOMT* (flavonoid 3'-O-methyltransferase), *CHI*, *COMT*1, and *COMT*6 (Fig. 4d). When the DAFs and DEGs in flavonoid biosynthesis were mapped to the KEGG metabolism pathways, we found that there were three different regulation models (DK, DL, and AEX) of flavonoid synthesis responding to drought stress (Fig. 5). Combining with Figure 4, 4 critical DEGs in flavonoid biosynthesis pathway shared among the three ecotypes, including *CHI*, *FLS* (flavonol synthase), *CYP*75*B*1, and *ANR*. To be mentioned, the flavonoid biosynthesis showed diverse among ecotypes under drought stress, except for the shared DAFs, i.e., vitexin. In DK, dihydrokaempferol and dihydroquercetin significantly increased, and the route dihydrokaempferol-dihydroquercetin activated by *CYP*75*B*1 might enhance the adaptation to drought stress (Fig. 5a). In addition, apigenin was significantly positive regulated by *CHI* (P<0.050) in DL (Fig. 5b). This ecotype might activate the metabolic flux route naringeninapigenin-luteolin to respond to drought stress. In AEX, we found rutin and quercetin were positively regulated by *CHI* (P<0.050), whose metabolic flux redirected from route quercetin-isorhamnetin to quercetin-isoquercitrin-rutin accompanied by transcriptional suppression on *OMT* (O-methyltransferase) (Fig. 5c). However, in DK and AEX, isorhamnetin was oppositely regulated under drought stress, which significantly increased in DK and decreased in AEX under drought stress.

3.5 qRT-PCR validation of expression levels of the genes related to flavonoid biosynthesis

To further confirm the reliability and repeatability of the transcriptome data, we subjected 8 structural genes involved in the biosynthetic pathway of flavonoid to qRT-PCR analysis. The results showed that the relative expression of 7 genes was consistent with the corresponding FPKM values in the transcriptomic data (Fig. 6).

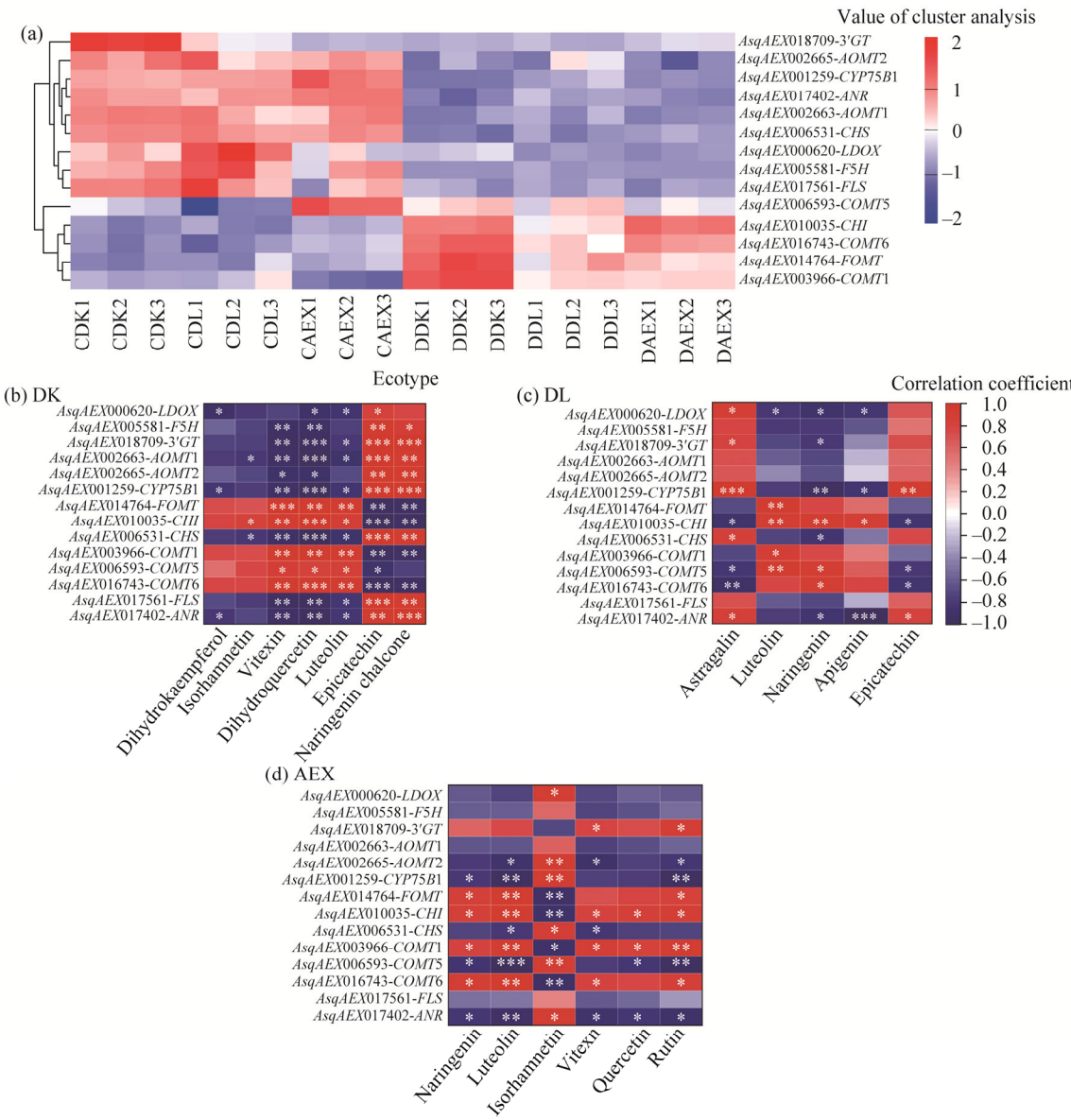

Fig. 4 Cluster analysis and correlation analysis between DEGs and differentially accumulated flavonoids (DAFs). (a), genes related to flavonoid synthesis in 18 samples. *LDOX*, leucoanthocyanidin dioxygenase; *F5H*, cytochrome P450 84A1; 3'*GT*, anthocyanin 3'-O-beta-glucosyltransferase; *AOMT*, flavonoid 3',5'-methyltransferase; *CYP75B1*, flavonoid 3'-monooxygenase; *FOMT*, flavonoid 3'-O-methyltransferase; *CHI*, chalcone isomerase; *CHS*, chalcone synthase; *COMT*, caffeic acid 3-O-methyltransferase; *FLS*, flavonol synthase; *ANR*, anthocyanidin reductase. (b–d), correlation analysis between DEGs and DAFs of DK (b), DL (c), and AEX (d). ***, **, and * represent significant differences at $P<0.001$, $P<0.010$, and $P<0.050$ levels, respectively. The abbreviations are the same in the following figures.

4 Discussion

Sandrice is regarded as a promising medicinal resource plant, which is widely endemic to arid and semi-arid desert areas. A common garden trial suggested that flavonoids accumulation differed among ecotypes of sandrice due to long-term local adaptation (Zhou et al. 2021a), and its accumulation was negatively correlated with the *in situ* precipitation across ecotypes (Fang et al., 2022). Hereby, with physiological traits, metabolomic profiles, and transcriptomic investigations under drought treatments on the three ecotypes of different amounts of precipitation (DK, DL,

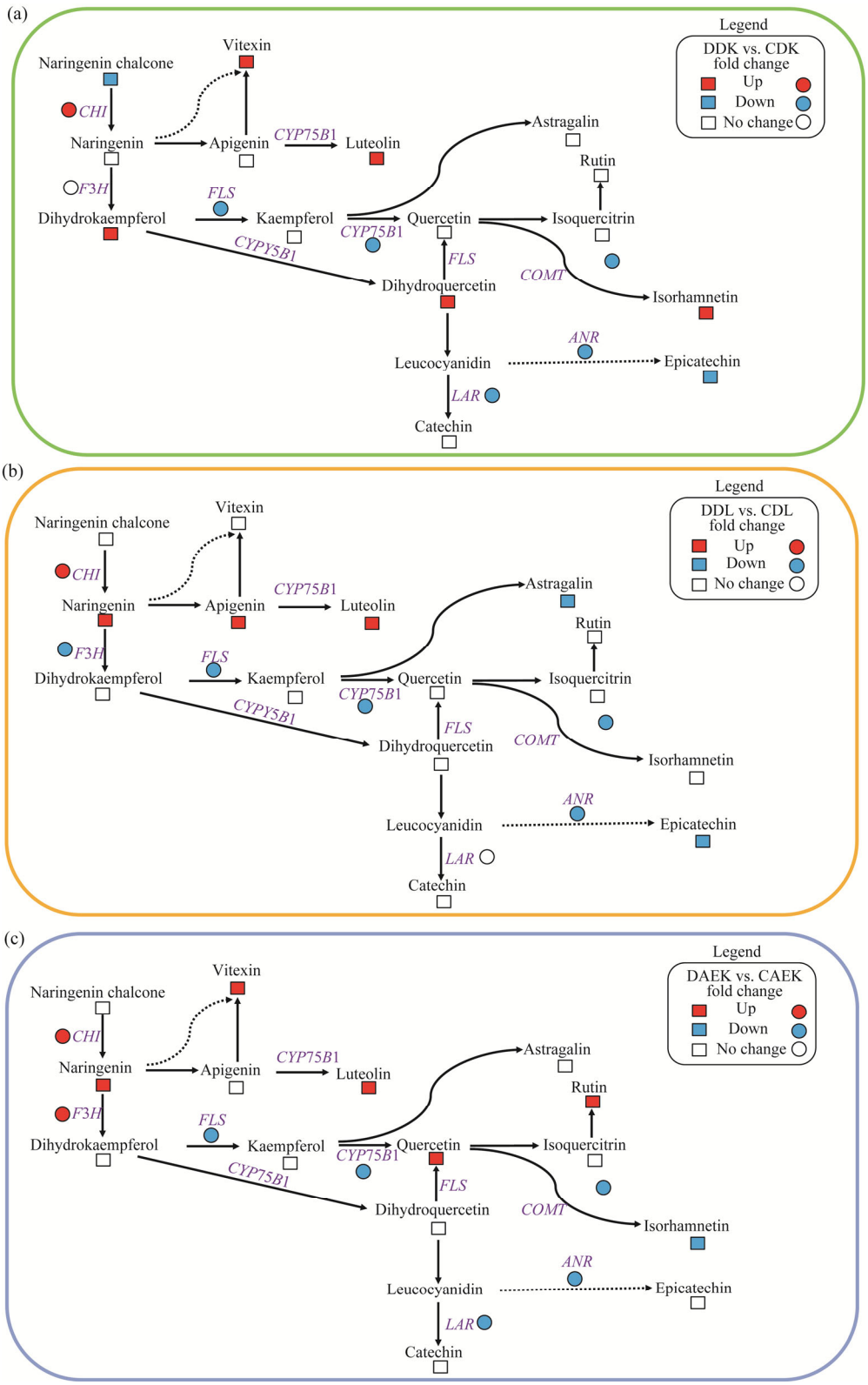

Fig. 5 Flavonoid biosynthesis pathway in response to drought stress in DK (a), DL (b), and AEX (c) ecotypes of sandrice. The heatmap colored red and blue indicates up-regulation and down-regulation of structural genes and flavonoid metabolites, respectively. The square and circle presented structural gene and flavonoid metabolites, respectively.

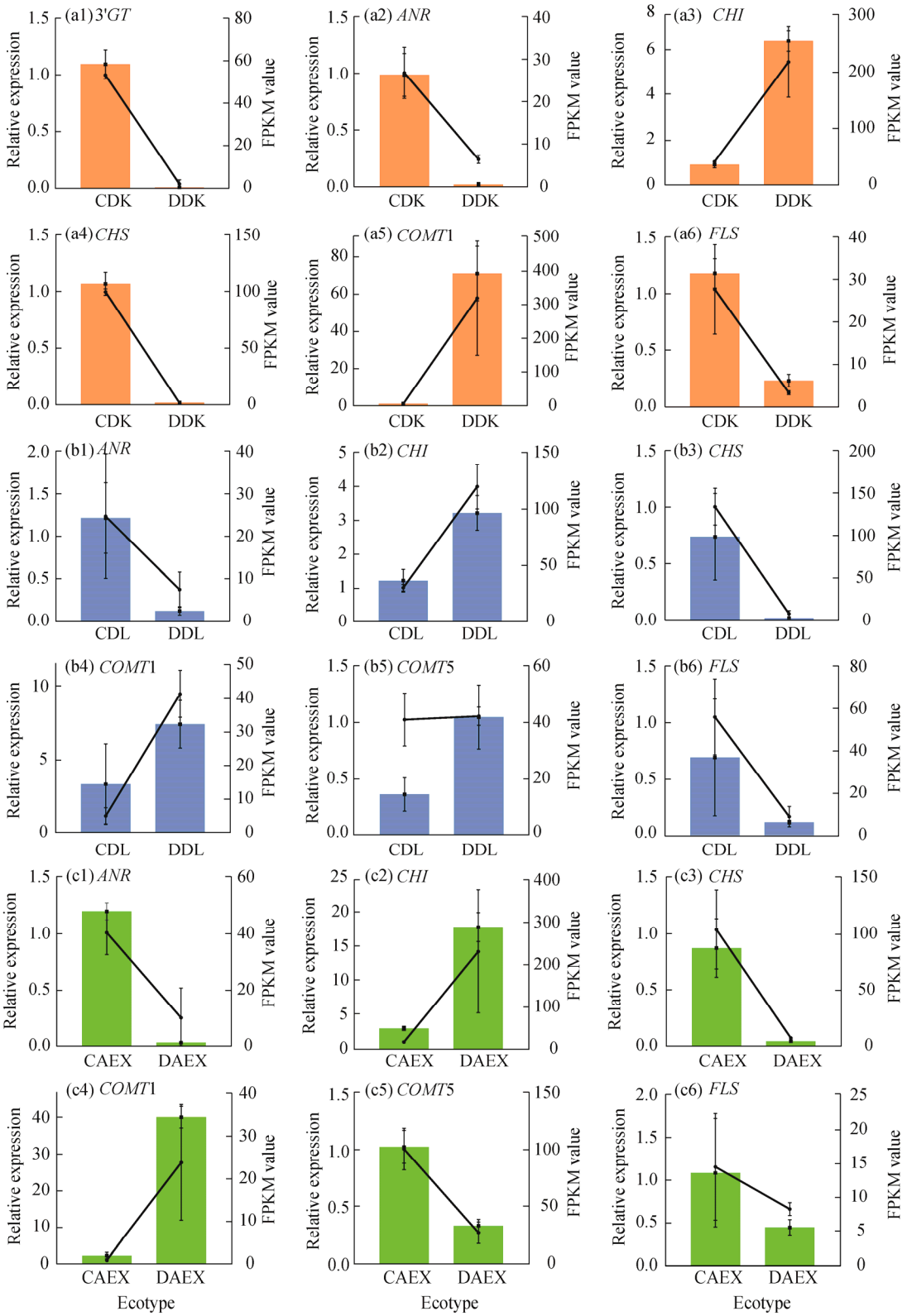

Fig. 6 Quantitative real-time polymerase chain reaction (qRT-PCR) validation of the transcriptome data in DK (a1–a6), DL (b1–b6) and AEX (c1–c6) ecotypes of sandrice. The line graph and the histogram with error bars present the relative expression calculated by the $2^{-\Delta\Delta Ct}$ method and fragments per kilobase million (FPKM) value generated by ribonucleic acid sequence (RNA-Seq), respectively.

and AEX), we tried to verify that the accumulation of flavonoid in sandrice was triggered by drought stress, and revealed the molecular metabolism regulation mechanism of flavonoid synthesis among different ecotypes. This study will support the precise utilization and development of this desert medicinal plant in the future. It also provides an example for the development of medicinal value of resource plants in desert arid areas, as well as theoretical support for the development of eco-agricultural health integration industry.

4.1 Differences of morphological and physiological responses to drought stress in sandrice

The morphological differences among sandrice ecotypes displayed significant local adaptation to precipitation (Yin et al., 2016a, b). In our study, we observed that the seedlings of sandrice exhibited the strong drought tolerance (4.00% soil moisture content) with short stature, collapsed structures, yellowing leaves, and wilting and curling after drought stress (Fig. 1a), similar to phenotypic responses observed in other species (Hu et al., 2021, 2022; Huang et al., 2023). Meanwhile, according to the fluorescence parameters (Fv'/Fm', a universal indicator of plant stress severity) (Sharma et al., 2015), we found that the departure of sandrice from its original habitat and its cultivation under laboratory conditions can be considered a form of stress due to inadequate light exposure. However, throughout the experiment, all conditions, except for the water content, were kept consistent between control and drought treatment groups. This consistency ensured the integrity and validity of drought treatment. Notably, sandrice in DL had the highest in PHI (Fig. 1d), LA (Fig. 1e), Fv'/Fm' (Fig. 1h), and leaf RWC (Fig. 1i) under drought stress, compared with DK and AEX. Conversely, sandrice in DK exhibited the lowest leaf RWC under drought conditions. Leaf RWC is one of the optimum indicators to reveal the water retention capacity of plants under drought-related stress, which is positively correlated with the drought resistance of plants (Karimpour, 2019). Within a plant species, in addition, the leaf RWC of drought sensitive genotype was generally lower than that of resistant genotype (Rampino et al., 2006). Our physiological results indicated that DL displayed greater drought resistance, while DK was more sensitive when facing the same drought environment. DL, the highest-altitude ecotype from Qinghai-Xizang Plateau, due to long-term adaptation to multiple stresses such as cold, ultraviolet B (UV-B), and drought, may develop stronger self-protection mechanisms responding to drought stress. Investigating the precipitation of native habitats, we found the annual mean precipitation of DL (263 mm) is twice that of DK (137 mm). In terms of the precipitation gradient, DK, the arid land ecotype, should be the most drought-tolerant ecotype. In addition, previous data showed that under drought conditions, the arid land ecotype exhibited a greater capacity for adaptation compared with the semi-arid land ecotype, further supporting this finding (Fang et al., 2023). However, based on the phenotypic changes of DK under drought treatment, it appeared that DK could be a drought-sensitive ecotype. It is reasonable to consider the original habitat of DK, located near the Yellow River with abundant groundwater. The physiological traits of DK include short, broad leaf (Table 1), and a fragile photosynthetic system (Fig. 1h), which may be not detrimental to the plant's ability to adapt to drought stress, especially when compared with the sandrice ecotypes with above-ground characteristics such as smaller, thicker leaves, and more robust photoprotective systems (Fang and Xiong, 2015; Bhusal et al., 2021). Thus, to elucidate the molecular mechanism of sandrice adaptation to drought stress, it is essential to conduct more detailed studies on root development under drought treatment across more ecotypes.

4.2 Rutin accumulation might contribute to drought stress responses in sandrice

The analysis of 15 flavonoid-targeting metabolites revealed that rutin, isoquercitrin, and astragalin were highly enriched in the above-ground tissues of sandrice, collectively accounting for more than 95.00% of the total 15 flavonoids (Fig. 2a). Numerous studies have demonstrated that rutin, isoquercitrin, and astragalin have a number of pharmacological effects, such as antimicrobial effects, anti-allergic activity, antioxidants, cardiovascular disorders, diabetes, cardioprotective properties, neuroprotective effects, anti-cancer, anti-inflammatory, and allergic reactions (Valentova et al., 2014; Ganeshpurkar and Saluja, 2017; Riaz et al., 2018; Resham et al., 2020; Negahdari et al., 2021). These results further supported the finding that above-ground

tissues of sandrice contain large amounts of flavonoids with outstanding medicinal value under current culture conditions. Rutin, the most abundant compound, was 1231.57–2859.34 ng/100 mg FW (equivalent to 61.60–143.00 μg/g dry weight (DW)) (Table 2). This result contradicted with a previous study that found the content of isorhamnetin was the highest (557.50 μg/g DW) in sandrice from the common garden trial (Zhou et al., 2021a). The common garden trial was conducted outdoors on plots with relatively high sand content in Wuwei City, Gansu Province, China. Throughout the entire growth period, there was ample sunlight, and environmental factors such as temperature and humidity fluctuated greatly. However, the present study utilized pure sand from the field mixed with nutrient soil, and the experiment was conducted under artificially simulated climatic conditions. During the cultivation period, environmental factors like temperature and humidity remained stable. Although the light intensity was lower than natural sunlight, it was still sufficient to meet the requirements of drought treatment experiments. In summary, the common garden trial and the controlled experiments differed significantly in terms of planting soil, nutritional status, climate, and other factors. Therefore, we propose that the variations in cultivation conditions may be the primary factors contributing to the differences in flavonoid accumulation between the common garden trial and the ambient drought treatment experiment. In fact, this kind of phenomenon has been observed in other plants as well, where number and content of plant flavonoids are easily influenced by their growing environment (Jaakola and Hohtola, 2010; Shi et al., 2022).

In the present study, the content of rutin in the three ecotypes increased under drought stress, indicating its accumulation was conducive to the response to drought stress (Fig. 2a). A previous study has shown rutin accumulation in the cytosol scavenges hydroxyl radicals produced in response to salinity stress in quinoa (*Chenopodium quinoa* Willd.), which belongs to the same family as sandrice (Ismail et al., 2015). Furthermore, research on *Fagopyrum tataricum* (L.) Gaertn. also confirmed that the high expression of encoded rutin biosynthetic enzymes and the accumulation of rutin contributed to improving tolerance to abiotic stress (Zhang et al., 2017). Those results suggested that the accumulation of rutin might contribute to scavenging ROS and enhance sandrice adaptability to drought stress. In addition, the common garden experiments also demonstrated the high content of rutin (Zhou et al., 2021b; Fang et al., 2022), indicating that rutin might be involved into the adaptation to the extreme environment in sandrice. In future work, it will still need an in-depth experiment such as applying exogenous rutin to leaves to further confirm whether it enhances drought tolerance in sandrice.

4.3 Diversity of flavonoid for local adaptation in sandrice

The secondary metabolites accumulated in sandrice may also exhibit diversity in response to stressful environments. Multi-omics integration analysis of flavonoid synthesis pathways showed the diversity of flavonoid accumulation among the three ecotypes of sandrice when responding to drought stress. DK might activate the metabolic flux route dihydrokaempferol-dihydroquercetin in adapting to drought stress (Fig. 5a). DL might activate the metabolic flux route naringenin-apigenin-luteolin in responding to drought stress (Fig. 5b). AEX might redirect metabolic flux from route quercetin-isorhamnetin to route quercetin-isoquercitrin-rutin by transcriptional suppression on *OMT* (Fig. 5c). Metabolic flux redirection is a common response in plants (Dong et al., 2020), as observed in our previous study on sandrice when exposed to *in situ* environmental differentiation among ecotypes (Fang et al., 2022). The reason of redirection in sandrice remains unclear, but the unusually high accumulation of some flavonoids might readjust the homeostasis to cope with drought stress. Studies in *Achillea pachycephala* Rech.f. (Gharibi et al., 2019) and *Chrysanthemum morifolium* (L.) Ramat. (Hodaei et al., 2018) have shown that water stress can stimulate the synthesis of apigenin and luteolin, accompanied with the up-regulation of their biosynthesis-related genes (*CHI*, *CHS*, and *F3H*) to enhance the ability to adapt to drought stress. Some researches have reported that quercetin is a key intermediate metabolite of flavonoid biosynthesis pathway to enhance drought tolerance (Yeloojeh et al., 2020; Singh et al., 2021), and this kind of phenomenon was also found in the ecotype AEX of sandrice under drought treatment.

Additionally, the accumulation of flavonoids in sandrice also exhibited variability across different ecotypes under cold stress. Specifically, our recent research revealed that AEX and DL demonstrated a higher phytochemical diversity when coping with low temperature, compared with DK (Zhao et al., 2024). This, together with the drought treatment results, suggest that the diversity of flavonoid accumulation patterns is ubiquitous among sandrice ecotypes with diverse environmental conditions. Although the flavonoid accumulation observed in this research was a consequence of genotype and environment interactions (Hodaei et al., 2018), the significant genetic differentiation was found between central lineage (DK and DL) and eastern lineage (AEX) in sandrice, which were also geographically differed in annual mean precipitation (Qian et al., 2016, 2021). However, the upstream part of the biosynthesis pathway of flavonoids was triggered by drought in DL, differed to DK that belongs to the same genetic lineage. Considering to environmental characteristics of DL, which came from Qinghai-Xizang Plateau, plants from DL endures not only drought but also the other stressors such as low temperature and UV-B. Thus, we proposed that the downstream part of the flavonoid biosynthesis could be more or less involved into adaptation to UV-B radiation and/or cold temperature. Actually, the downstream flavonoids such as dihydroquercetin, isorhamnetin, kaempferol, and quercetin, were witnessed to be significantly accumulated under cold treatment in DL (Zhao et al., 2024). In this case, we would conclude that the phytochemistry diversity of flavonoids among sandrice ecotypes could be the consequences of local adaptation to the combination of multiple stresses across different deserts. In the future, it is essential to undertake a series of combined stress experiments to delve deeper into the molecular metabolic mechanisms of sandrice adaptation to multiple stresses (Jansen et al., 2021; Jan et al., 2022).

5 Conclusions

The present study conducted a preliminary analysis, which determined that drought stress triggered the flavonoid accumulation in sandrice. It also revealed that sandrice could fine-tune the synthesis of flavonoids across different ecotypes in response to drought stress. The three ecotypes responded to drought stress by activating different flavonoid biosynthesis pathways, displaying diversification of flavonoid metabolites accumulation among ecotypes. This work provides valuable germplasm resources and evaluation methods for the acclimation of medicinal sandrice, and is of significance to the research of non-model plants response to drought stress. In the future, there still needs to be further research to deeply elucidate the molecular mechanism of how drought affects the sandrice flavonoid synthesis by combining more omics methods, including genomics and proteomics.

Conflict of interest

The authors declare that they have no known competing financial interests or personal relationships that could have appeared to influence the work reported in this paper.

Acknowledgements

This research was financially supported by the National Natural Science Foundation of China (32271695), the Science and Technology Program of Gulang County, Gansu Province (GL2302YFN006), the Youth Science and Technology Talent Innovation Project of Lanzhou City (2023-QN-140), the Strategic Biological Resources Program of Chinese Academy of Sciences (KFJ-BRP-007-015), and the Development of Scientific and Technological Innovation Special Fund Competitive Project of Gansu Province (Y939BD1001).

Author contributions

Experimental work: ZHAO Pengshu; Methodology: ZHAO Pengshu; Software, sample analysis, and data analysis: ZHAO Pengshu; Writing - original draft preparation: ZHAO Pengshu; Funding acquisition: MA Xiaofei, YAN Xia, QIAN Chaoju; Supervision: MA Xiaofei, YAN Xia, QIAN Chaoju; Conceptualization and design: MA

Xiaofei; Project administration: MA Xiaofei; Funding acquisition and experimental support: MA Guorong; Writing- reviewing and editing: YAN Xia, QIAN Chaoju, FANG Tingzhou, YIN Xiaoyue, ZHOU Shanshan, LIAO Yuqiu, SHI Liang, FAN Xingke, Awuku IBRAHIM, MA Xiaofei. All authors approved the manuscript.

References

Agati G, Azzarello E, Pollster S, et al. 2012. Flavonoids as antioxidants in plants: Location and functional significance. Plant Science, 196: 67–76.

Basu S, Ramegowda V, Kumar A, et al. 2016. Plant adaptation to drought stress. F1000Res, 5: 1554, doi: 10.12688/f1000research.7678.1.

Bhusal N, Lee M, Lee H, et al. 2021. Evaluation of morphological, physiological, and biochemical traits for assessing drought resistance in eleven tree species. Science of the Total Environment, 779: 146466, doi: 10.1016/j.scitotenv.2021.146466.

Dong N Q, Sun Y W, Guo T, et al. 2020. UDP-glucosyltransferase regulates grain size and abiotic stress tolerance associated with metabolic flux redirection in rice. Nature Communication, 11(1): 2629, doi: 10.1038/s41467-020-16403-5.

Easterling D R, Meehl G A, Parmesan C, et al. 2000. Climate extremes: Observations, modeling, and impacts. Science, 289(5487): 2068–2074.

Fang T Z, Zhou S S, Qian C J, et al. 2022. Integrated metabolomics and transcriptomics insights on flavonoid biosynthesis of a medicinal functional forage, *Agriophyllum squarrosum* (L.), based on a common garden trial covering six ecotypes. Frontiers in Plant Science, 13: 985572, doi: 10.3389/fpls.2022.985572.

Fang T Z, Qian C J, Daoura B G, et al. 2023. A novel TF molecular switch-mechanism found in two contrasting ecotypes of a psammophyte, *Agriophyllum squarrosum*, in regulating transcriptional drought memory. BMC Plant Biology, 23: 167, doi: 10.1186/s12870-023-04154-6.

Fang Y J, Xiong L Z. 2015. General mechanisms of drought response and their application in drought resistance improvement in plants. Cellular and Molecular Life Sciences, 72: 673–689.

Ganeshpurkar A, Saluja A K. 2017. The pharmacological potential of rutin. Saudi Pharmaceutical Journal, 25(2): 149–164.

Gao G R, Lv Z R, Zhang G Y, et al. 2021. An ABA–flavonoid relationship contributes to the differences in drought resistance between different sea buckthorn subspecies. Tree Physiology, 41(5): 744–755.

Gao Y G, Jin Y L, Guo W, et al. 2022. Metabolic and physiological changes in the roots of two oat cultivars in response to complex saline-alkali stress. Frontiers in Plant Science, 13: 835414, doi: 10.3389/fpls.2022.835414.

Gautam H, Sharma A, Trivedi P K. 2023. The role of flavonols in insect resistance and stress response. Current Opinion in Plant Biology, 73: 102353, doi: 10.1016/j.pbi.2023.102353.

Gharibi S, Tabatabaei B E S, Saeidi G, et al. 2019. The effect of drought stress on polyphenolic compounds and expression of flavonoid biosynthesis related genes in *Achillea pachycephala* Rech.f. Phytochemistry, 162: 90–98.

Ghorbanpour M, Varma A. 2017. Medicinal Plants and Environmental Challenges. Switzerland: Springer, 259–277.

Hao Z C, Hao F H, Singh V P, et al. 2018. Changes in the severity of compound drought and hot extremes over global land areas. Environmental Research Letters, 13: 124022, doi: 10.1088/1748-9326/aaee96.

Hodaei M, Rahimmalek M, Arzani A, et al. 2018. The effect of water stress on phytochemical accumulation, bioactive compounds and expression of key genes involved in flavonoid biosynthesis in *Chrysanthemum morifolium* L. Industrial Crops and Products, 120: 295–304.

Hou G D, Li S, Shang C Q, et al. 2022. Genome-wide characterization of chalcone synthase genes in sweet cherry and functional characterization of *CpCHS*1 under drought stress. Frontiers in Plant Science, 13: 989959, doi: 10.3389/fpls.2022.989959.

Hu H C, Fei X T, He B B, et al. 2021. Integrated analysis of metabolome and transcriptome data for uncovering flavonoid components of *Zanthoxylum bungeanum* Maxim. leaves under drought stress. Frontiers in Nutrition, 8: 801244, doi: 10.3389/fnut.2021.801244.

Hu H C, Liu Y H, He B B, et al. 2022. Integrative physiological, transcriptome, and metabolome analysis uncovers the drought responses of two *Zanthoxylum bungeanum* cultivars. Industrial Crops and Products, 189: 115812, doi: 10.1016/j.indcrop.2022.115812.

Huang X, Chu G M, Wang J, et al. 2023. Integrated metabolomic and transcriptomic analysis of specialized metabolites and isoflavonoid biosynthesis in *Sophora alopecuroides* L. under different degrees of drought stress. Industrial Crops and Products, 197: 116595, doi: 10.1016/j.indcrop.2023.116595.

Ismail H, Maksimovic J D, Maksimovic V, et al. 2015. Rutin, a flavonoid with antioxidant activity, improves plant salinity tolerance by regulating K^+ retention and Na^+ exclusion from leaf mesophyll in quinoa and broad beans. Functional Plant

Biology, 43(1): 75–86.

Jaakola L, Hohtola A. 2010. Effect of latitude on flavonoid biosynthesis in plants. Plant, Cell and Environment, 33(8): 1239–1247.

Jan R, Khan M, Asaf S, et al. 2022. Drought and UV radiation stress tolerance in rice is improved by over accumulation of non-enzymatic antioxidant flavonoids. Antioxidants, 11(5): 917, doi: 10.3390/antiox11050917.

Jansen M A K, Ač A, Klem K, et al. 2021. A meta-analysis of the interactive effects of UV and drought on plants. Plant, Cell and Environment, 45(1): 41–54.

Karimpour M. 2019. Effect of drought stress on RWC and chlorophyll content on wheat (*Triticum durum* L.) genotypes. World Essays Journal, 7(1): 52–56.

Kim Y H, Khan A L, Waqas M, et al. 2017. Silicon regulates antioxidant activities of crop plants under abiotic-induced oxidative stress: A review. Frontiers in Plant Science, 8: 510, doi: 10.3389/fpls.2017.00510.

Li B Z, Fan R N, Sun G L, et al. 2021. Flavonoids improve drought tolerance of maize seedlings by regulating the homeostasis of reactive oxygen species. Plant and Soil, 461: 389–405.

Li J Y, Wei J H, Song Y T, et al. 2023. Histone H3K9 acetylation modulates gene expression of key enzymes in the flavonoid and abscisic acid pathways and enhances drought resistance of sea buckthorn. Physiologia Plantarum, 175(3): e13936, doi: 10.1111/ppl.13936.

Lu M N, He W J, Xu Z Y, et al. 2023. The effect of high altitude on ephedrine content and metabolic variations in two species of Ephedra. Frontiers in Plant Science, 14: 1236145, doi: 10.3389/fpls.2023.1236145.

Lv H W, Wang Q L, Luo M, et al. 2023. Phytochemistry and pharmacology of natural prenylated flavonoids. Archives of Pharmacal Research, 46(4): 207–272.

Negahdari R, Bohlouli S, Sharifi S, et al. 2021. Therapeutic benefits of rutin and its nanoformulations. Phytotherapy Research, 35(4): 1719–1738.

Prasad P V V, Pisipati S R, Momčilović I, et al. 2011. Independent and combined effects of high temperature and drought stress during grain filling on plant yield and chloroplast EF-Tu expression in spring wheat. Journal of Agronomy and Crop Science, 197(6): 430–441.

Qian C J, Yin H X, Shi Y, et al. 2016. Population dynamics of *Agriophyllum squarrosum*, a pioneer annual plant endemic to mobile sand dunes, in response to global climate change. Scientific Reports, 6: 26613, doi: 10.1038/srep26613.

Qian C J, Yan X, Fang T Z, et al. 2021. Genomic adaptive evolution of sand rice (*Agriophyllum squarrosum*) and its implications for desert ecosystem restoration. Frontiers in Genetics, 12: 656061, doi: 10.3389/fgene.2021.656061.

Rampino P, Pataleo S, Gerardi C, et al. 2006. Drought stress response in wheat: Physiological and molecular analysis of resistant and sensitive genotypes. Plant, Cell and Environment, 29(12): 2143–2152.

Resham K, Khare P, Bishnoi M, et al. 2020. Neuroprotective effects of isoquercitrin in diabetic neuropathy via Wnt/beta-catenin signaling pathway inhibition. Biofactors, 46(3): 411–420.

Riaz A, Rasul A, Hussain G, et al. 2018. Astragalin: A bioactive phytochemical with potential therapeutic activities. Advances Pharmacological Sciences, 2018: 979462515, doi: 10.1155/2018/9794625.

Samanta A, Das G, Das S K. 2011. Roles of flavonoids in plants. International Journal of Pharmaceutics, 6(1): 12–35.

Sharma D K, Andersen S B, Ottosen C O, et al. 2015. Wheat cultivars selected for high Fv/Fm under heat stress maintain high photosynthesis, total chlorophyll, stomatal conductance, transpiration and dry matter. Physiologia Plantarum, 153(2): 284–298.

Shen N, Wang T F, Gan Q, et al. 2022. Plant flavonoids: Classification, distribution, biosynthesis, and antioxidant activity. Food Chemistry, 383: 132531, doi: 10.1016/j.foodchem.2022.132531.

Shi Y S, Yang L, Yu M F, et al. 2022. Seasonal variation influences flavonoid biosynthesis path and content, and antioxidant activity of metabolites in *Tetrastigma hemsleyanum* Diels & Gilg. PloS ONE, 17(4): e0265954, doi: 10.1371/journal.pone.0265954.

Shomali A, Das S, Arif N, et al. 2022. Diverse physiological roles of flavonoids in plant environmental stress responses and tolerance. Plants, 11(22): 3158, doi: 10.3390/plants11223158.

Singh P, Arif Y, Bajguz A, et al. 2021. The role of quercetin in plants. Plant Physiology and Biochemistry, 166: 10–19.

Sun S C, Xiong X P, Zhang X L, et al. 2020. Characterization of the *Gh4CL* gene family reveals a role of *Gh4CL7* in drought tolerance. BMC Plant Biology, 20: 125, doi: 10.1186/s12870-020-2329-2.

Valentova K, Vrba J, Bancirova M, et al. 2014. Isoquercitrin: Pharmacology, toxicology, and metabolism. Food and Chemical Toxicology, 68: 267–282.

Wang A M, Zhu M K, Luo Y H, et al. 2017. A sweet potato cinnamate 4-hydroxylase gene, *IbC4H*, increases phenolics content and enhances drought tolerance in tobacco. Acta Physiologiae Plantarum, 39: 276, doi: 10.1007/s11738-017-2551-1.

Xie Y Y, Wang X J, Silander J A. 2015. Deciduous forest responses to temperature, precipitation, and drought imply complex climate change impacts. Proceedings of the National Academy of Sciences of the United States of America, 112(44): 13585–13590.

Yadav B, Jogawat A, Rahman M S, et al. 2021. Secondary metabolites in the drought stress tolerance of crop plants: A review. Gene Reports, 23: 101040, doi: 10.1016/j.genrep.2021.101040.

Yang Z R, Cao Y B, Shi Y T, et al. 2023. Genetic and molecular exploration of maize environmental stress resilience: Towards sustainable agriculture. Molecular Plant, 16(10): 1496–1517.

Yeloojeh K A, Saeidi G, Sabzalian M R. 2020. Drought stress improves the composition of secondary metabolites in safflower flower at the expense of reduction in seed yield and oil content. Industrial Crops and Products, 154: 112496, doi: 10.1016/j.indcrop.2020.112496.

Yin C L, Zhao J C, Hu J L, et al. 2016a. Phenotypic variation of a potential food crop, *Agriophyllum squarrosum*, impacted by environmental heterogeneity. Scientia Sinica Vitae, 46(11): 1324–1335. (in Chinese)

Yin C L, Qian C J, Chen G X, et al. 2016b. The influence of selection of ecological differentiation to the phenotype polymorphism of *Agriophyllum squarrosum*. Journal of Desert Research, 36(2): 364–373. (in Chinese)

Yin X Y, Wang W D, Qian C J, et al. 2018. Analysis of metabolomics in *Agriophyllum squarrosum* based on UPLC-MS. Chinese Journal of Experimental Traditional Medical Formulae, 24(15): 51–56. (in Chinese)

Zhang L J, Li X X, Ma B, et al. 2017. The tartary buckwheat genome provides insights into rutin biosynthesis and abiotic stress tolerance. Molecular Plant, 10(9): 1224–1237.

Zhao P S, Shi L, Yan X, et al. 2023. Long-term feeding of sand rice (*Agriophyllum squarrosum* seed) can improve the antioxidant capacity of mice. Research in Cold and Arid Regions, 15(2): 105–112.

Zhao P S, Yan X, Qian C J, et al. 2024. Flavonoid synthesis pathway response to low-temperature stress in a desert medicinal plant, *Agriophyllum squarrosum* (sandrice). Genes, 15(9): 1228, doi: 10.3390/genes15091228.

Zhou S S, Yan X, Yang J, et al. 2021a. Variations in flavonoid metabolites along altitudinal gradient in a desert medicinal plant *Agriophyllum squarrosum*. Frontiers in Plant Science, 12: 683265, doi: 10.3389/fpls.2021.683265.

Zhou S S, Yang J, Qian C J, et al. 2021b. Organic acid metabolites involved in local adaptation to altitudinal gradient in *Agriophyllum squarrosum*, a desert medicinal plant. Journal of Plant Research, 134: 999–1011.

Appendix

Table S1 Primers for quantitative real-time PCR (qRT-PCR) analysis

Gene name	Gene No.	Forward primer (5′ to 3′)	Reverse primer (5′ to 3′)	Primer melting temperature (°C)	Product length (bp)
UBC22	*AsqAEX*016065	AATGGAGCCCAGCACTTACA	GCCTCATACTTTGGCCGATCA	57.00	133
PP2A	*AsqAEX*007496	TCGCCCCTGTTTAGTGGAGT	GTACGTCTTCTCTGCCGACT	58.00	122
3′GT	*AsqAEX*018709	TAGCAAAGCTCTGGGCATCC	GTGAGTCTATGGAGTCGCGG	58.00	90
CYP75B1	*AsqAEX*001259	CGGAGGTGCTAAAGAAGGCA	GACTACAGGGTGCAAACGGA	58.00	137
ANR	*AsqAEX*017402	ACTCCCAGCCCTAACTGCTA	CTCCACCCCAGCTACTGTTG	58.00	132
CHS	*AsqAEX*006531	GGGGTCAGCCCAAGTCTAAG	TTGGTGAGTTGGTAGTCCGC	58.00	88
FLS	*AsqAEX*017561	GACTGGGGCTGCAAGAAGAT	ATCAGGGCAAGGACATGGTG	58.00	101
COMT5	*AsqAEX*006593	CTACAGAATCCGGATGCCCC	CGACTGTGCGAACTGTTGTG	58.00	94
COMT1	*AsqAEX*003966	GCACATTTGCCAGCCAAGAA	GGTCCTGATGGTGCAAGTGA	58.00	99
CHI	*AsqAEX*010035	TCTGGAAGGCCATCGGAGTA	AAAATAGAGTGGCCCGGTGG	58.00	103

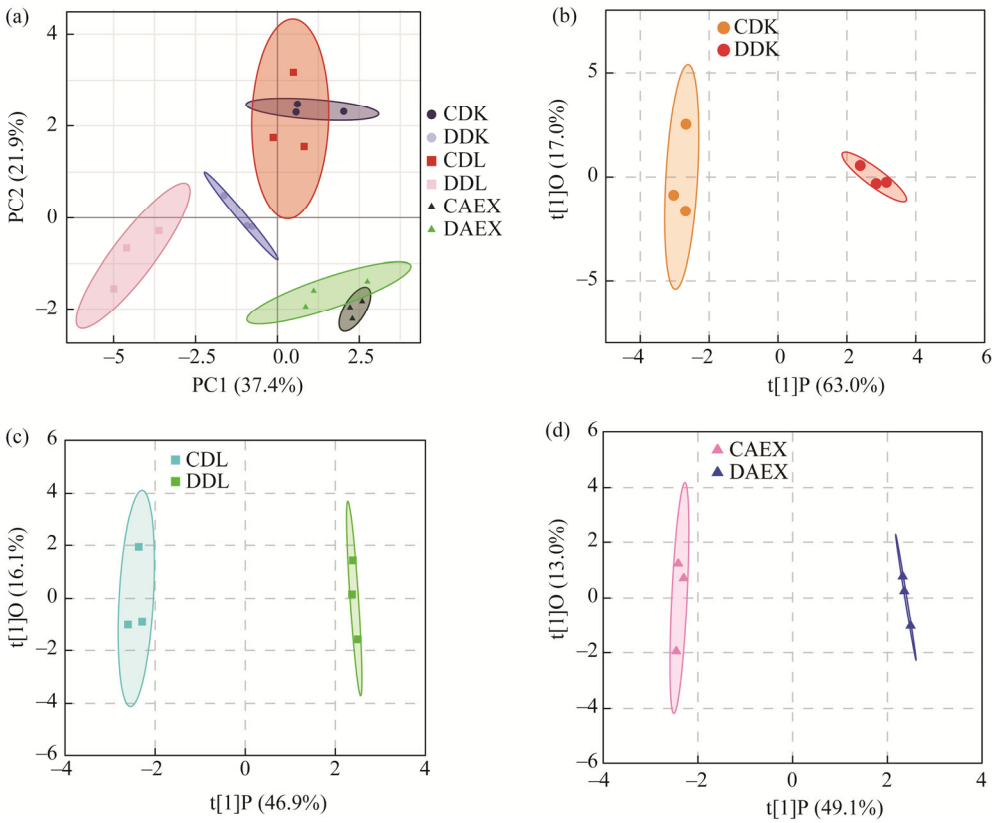

Fig. S1 Significant difference analysis of flavonoid-targeting metabolites in above-ground tissue of sandrice. (a), principal component analysis (PCA); (b–d), orthogonal partial least squares discriminant analysis (OPLS-DA). PC1 represents the first principal component, and PC2 represents the second principal component. t[1]P represents the predicted principal component score of the first principal component, showing the differences between sample groups, and t[1]O represents the orthogonal principal component score of the second principal component, showing the differences within sample groups.

Table S2 Summary of the ribonucleic acid sequence (RNA-Seq) results of sandrice aboveground tissue

Sample	Raw data (Gb)	Clean data (Gb)	Q30 (%)	Uniquely mapped (%)	Total mapped reads (%)	GC (%)
CDK1	7.09	6.68	91.05	93.16	96.25	44.78
CDK2	7.21	6.71	91.20	93.53	96.38	45.21
CDK3	7.61	7.08	90.87	93.21	96.11	45.09
DDK1	6.83	6.38	90.69	92.19	95.72	44.37
DDK2	6.91	6.47	90.55	92.23	95.68	44.25
DDK3	6.93	6.45	90.77	92.48	95.78	44.43
CDL1	7.01	6.63	91.91	93.40	96.22	45.28
CDL2	6.66	6.22	91.92	93.45	96.17	45.12
CDL3	7.41	6.95	91.04	93.06	95.89	44.68
DDL1	7.32	6.91	91.32	92.52	95.71	44.47
DDL2	7.63	7.19	91.21	92.57	95.87	44.37
DDL3	7.29	6.88	91.57	92.68	96.16	44.38
CAEX1	7.14	6.57	91.50	94.72	97.76	44.96
CAEX2	7.11	6.70	91.32	94.56	97.55	44.94
CAEX3	7.12	6.75	91.50	94.69	97.79	44.71
DAEX1	7.34	6.87	91.22	94.39	97.78	44.37
DAEX2	6.97	6.47	90.54	93.87	97.04	44.56
DAEX3	6.97	6.53	90.78	94.34	97.62	44.49

Note: Q30 is the percentage of bases with a mass value greater than or equal to 30, and the higher the value, the better the quality of the sequencing. GC content refers to the total proportion of guanine (G) and cytosine (C) bases in a DNA sequence, usually expressed as a percentage. DK, Dengkou County; DL, Dulan County; AEX, Aerxiang Village. CDK, CDL, CAEX are the control treatments of DK, DL, and AEX, respectively; DDK, DDL, and DAEX are the drought stress treatments of DK, DL and AEX, respectively.

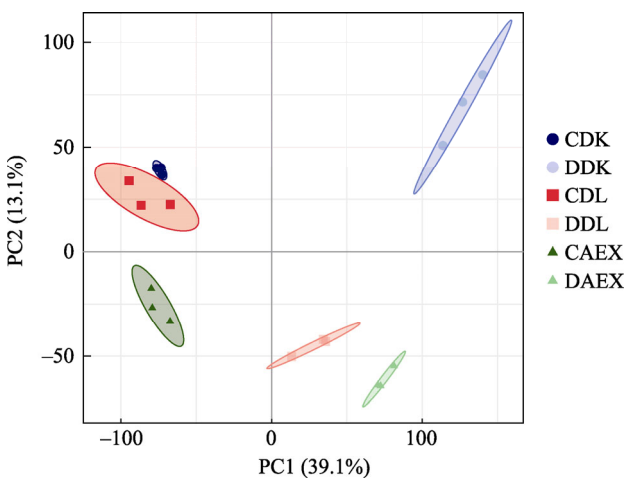

Fig. S2 PCA analysis showing the transcriptomes divergence

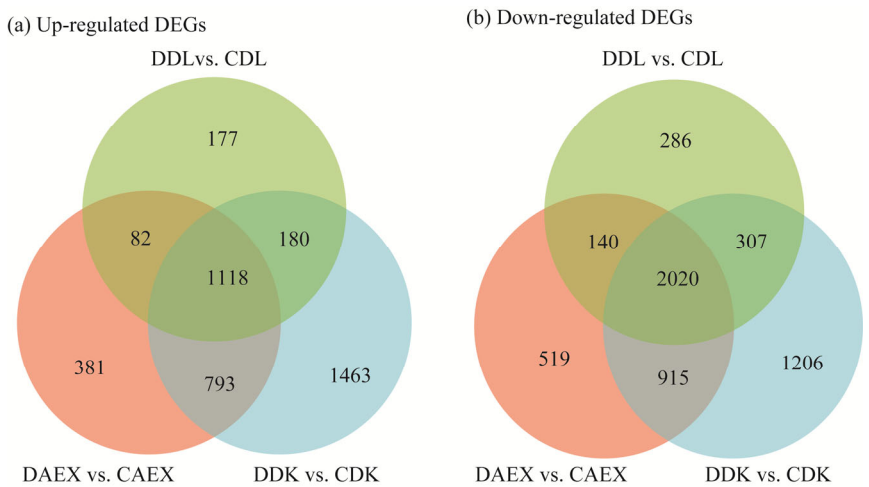

Fig. S3 Venn diagram showing overlap of up-regulated differentially expressed genes (DEGs) (a) and down-regulated DEGs (b) in the three ecotypes

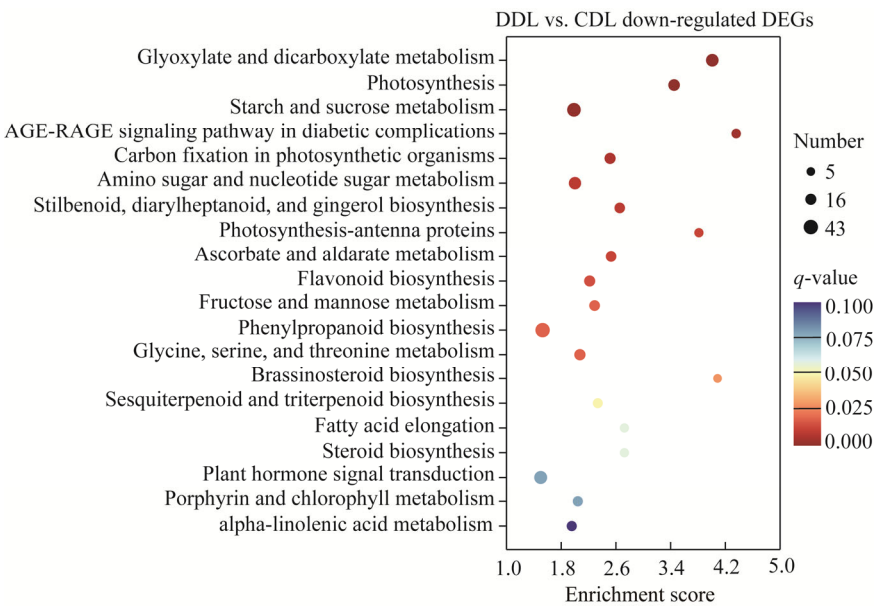

Fig. S4 Kyoto encyclopedia of genes and genomes (KEGG) enrichment analysis bubble map in DL. AGE-RAGE, advanced glycation end products-receptor for advanced glycation end products.